

## Telescope Array Experiment

H. Kawai<sup>a</sup>, S. Yoshida<sup>a</sup>, H. Yoshii<sup>b</sup>, K. Tanaka<sup>c</sup>, F. Cohen<sup>d</sup>, M. Fukushima<sup>d</sup>, N. Hayashida<sup>d</sup>, K. Hiyama<sup>d</sup>, D. Ikeda<sup>d</sup>, E. Kido<sup>d</sup>, Y. Kondo<sup>d</sup>, T. Nonaka<sup>d</sup>, M. Ohnishi<sup>d</sup>, H. Ohoka<sup>d</sup>, S. Ozawa<sup>d</sup>, H. Sagawa<sup>d</sup>, N. Sakurai<sup>d</sup>, T. Shibata<sup>d</sup>, H. Shimodaira<sup>d</sup>, M. Takeda<sup>d</sup>, A. Taketa<sup>d</sup>, M. Takita<sup>d</sup>, H. Tokuno<sup>d</sup>, R. Torii<sup>d</sup>, S. Udo<sup>d</sup>, Y. Yamakawa<sup>d</sup>, H. Fujii<sup>e</sup>, T. Matsuda<sup>e</sup>, M. Tanaka<sup>e</sup>, H. Yamaoka<sup>e</sup>, K. Hibino<sup>f</sup>, T. Benno<sup>g</sup>, K. Doura<sup>g</sup>, M. Chikawa<sup>g</sup>, T. Nakamura<sup>h</sup>, M. Teshima<sup>i</sup>, K. Kadota<sup>j</sup>, Y. Uchihori<sup>k</sup>, K. Hayashi<sup>l</sup>, Y. Hayashi<sup>l</sup>, S. Kawakami<sup>l</sup>, T. Matsuyama<sup>l</sup>, M. Minamino<sup>l</sup>, S. Ogio<sup>l\*</sup>, A. Ohshima<sup>l</sup>, T. Okuda<sup>l</sup>, N. Shimizu<sup>l</sup>, H. Tanaka<sup>l</sup>, D.R. Bergman<sup>m</sup>, G. Hughes<sup>m</sup>, S. Stratton<sup>m</sup>, G.B. Thomson<sup>m</sup>, A. Endo<sup>n</sup>, N. Inoue<sup>n</sup>, S. Kawana<sup>n</sup>, Y. Wada<sup>n</sup>, K. Kasahara<sup>o</sup>, R. Azuma<sup>p</sup>, T. Iguchi<sup>p</sup>, F. Kakimoto<sup>p</sup>, S. Machida<sup>p</sup>, K. Misumi<sup>p</sup>, Y. Murano<sup>p</sup>, Y. Tameda<sup>p</sup>, Y. Tsunesada<sup>p</sup>, J. Chiba<sup>q</sup>, K. Miyata<sup>q</sup>, T. Abu-Zayyad<sup>r</sup>, J.W. Belz<sup>r</sup>, R. Cady<sup>r</sup>, Z. Cao<sup>r</sup>, P. Huentemeyer<sup>r</sup>, C.C.H. Jui<sup>r</sup>, K. Martens<sup>r</sup>, J.N. Matthews<sup>r</sup>, M. Mostofa<sup>r</sup>, J.D. Smith<sup>r</sup>, P. Sokolsky<sup>r</sup>, R.W. Springer<sup>r</sup>, J.R. Thomas<sup>r</sup>, S.B. Thomas<sup>r</sup>, L.R. Wiencke<sup>r</sup>, T. Doyle<sup>s</sup>, M.J. Taylor<sup>s</sup>, V.B. Wickwar<sup>s</sup>, T.D. Wilkerson<sup>s</sup>, K. Hashimoto<sup>t</sup>, K. Honda<sup>t</sup>, K. Ikuta<sup>t</sup>, T. Ishii<sup>t</sup>, T. Kanbe<sup>t</sup>, and T. Tomida<sup>t</sup>

<sup>a</sup>Chiba University, 1-33 Yayoi-cho, Inage-ku, Chiba, 263-8522, Japan

<sup>b</sup>Ehime University, 2-5 Bunkyo-cho, Matsuyama, Ehime, 790-8577, Japan

<sup>c</sup>Hiroshinma City University, 3-4-1 Ozuka-Higashi, Asa-Minami-ku, Hiroshima, 731-3194, Japan

<sup>d</sup>ICRR, University of Tokyo, 5-1-5 Kashiwanoha, Kashiwa, Chiba, 277-8582, Japan

<sup>e</sup>Institute of Particle and Nuclear Studies, KEK, 1-1 Oho, Tsukuba, Ibaraki, 305-0801, Japan

<sup>f</sup>Kanagawa University, 3-27-1 Rokkakubayashi, Kanagawa-ku, Yokohama, Kanagawa, 221-8686, Japan

<sup>g</sup>Kinki University, 3-4-1 Kowakae, Higashi-Osaka, Osaka, 577-8502, Japan

<sup>h</sup>Kochi University, 2-5-1 Akebono-cho, Kochi, 780-8520, Japan

<sup>i</sup>Max-Planck-Institute for Physics, Foehringer Ring 6, 80805 München, Germany

<sup>j</sup>Musashi Institute of Technology, 1-28-1 Tamazutsumi, Setagawa-ku, Tokyo, 158-8558, Japan

<sup>k</sup>National Institute of Radiological Sciences, 4-9-1 Anagawa Inage-ku, Chiba, 263-8555, Japan

<sup>l</sup>Osaka City University, 3-3-138 Sugimoto-cho, Sumiyoshi-ku, Osaka, 558-8585, Japan

<sup>m</sup>Rutgers University, 136 Freilinghuysen Road, Piscataway, NJ 08854, USA

<sup>n</sup>Saitama University, 255 Shimo-Okubo, Sakura-ku, Saitama, 338-8570, Japan

<sup>o</sup>Shibaura Institute of Technology, 307 Fukasaku, Minuma-ku, Saitama, 337-8570, Japan

<sup>p</sup>Tokyo Institute of Technology, 2-12-1 Ookayama, Meguro-ku, Tokyo, 152-8550, Japan

<sup>q</sup>Tokyo University of Science, 2641 Yamazaki, Noda, Chiba, 278-8510, Japan

<sup>r</sup>University of Utah, 115 S 1400 E, Salt Lake City, UT 84112, USA

<sup>s</sup>Utah State University, Logan, UT 84322, USA

<sup>t</sup>Yamanashi University, 4-4-37 Takeda, Kofu, Yamanashi, 400-8510, Japan

The TA observatory is a hybrid detector system consisting of both a surface detector array as well as a set of fluorescence detectors, and the observatory will measure the energy spectrum, anisotropy and composition of ultra-high energy cosmic rays. The Surface Detectors are being deployed and the array should be complete by the end of February, 2007. We will soon be collecting hybrid data at the Telescope Array.

## 1. Introduction

The Telescope Array (TA) Project[1] is designed to study cosmic rays with energies above  $10^{19}$  eV. The TA observatory will measure the energy spectrum, arrival direction distribution (anisotropy) and composition of Ultra-High Energy Cosmic Rays (UHECRs). It will look for the super-GZK events[2] and the event clusters[3] observed by AGASA (the Akeno Giant Air Shower Array) and will resolve the discrepancy between the AGASA results and those of HiRes (the High Resolution Fly’s Eye)[4].

The TA observatory is a hybrid detector system consisting of both a Surface Detector (SD) array (ala AGASA) as well as a set of Fluorescence Detectors (FD) (ala HiRes). A map of the observatory is shown in Figure 1, *i.e.*, it consists of 576 scintillation Surface Detectors (SDs) which measure the distribution of charged particles at the Earth’s surface and three Fluorescence Detector (FD) stations which observe the night sky above the SD array[5]. The SD array covers an area nine times greater than the AGASA detection area. We can observe both the longitudinal development and the lateral distribution of air showers simultaneously with the hybrid system. Thus, we will use the measured parameters for complementary calibrations and can improve the energy and the angular resolutions of each component of the hybrid system.

The TA observatory is located in Millard County, Utah, USA ( $39.1^{\circ}\text{N}$ ,  $112.9^{\circ}\text{W}$ ). The site is about 1400 m above sea level. As with the AGASA and HiRes experiments, the TA observatory is located in the northern hemisphere. This allows the TA to directly compare with AGASA and HiRes measurement and to compare with southern experiments to search for a potential north-south asymmetry in energy spectra or source distribution.

We chose scintillation detectors for the SD array of TA experiment, because scintillators have a smaller systematic error in the primary energy determination when compared to a water tank SD array. This is because, for UHECRs, about 90% of the energy of the primary particle is con-

verted to electro-magnetic component in the atmosphere, and because the lateral particle density distribution of electrons has a smaller dependence on hadron interaction models[6] and on primary species than that of muons.

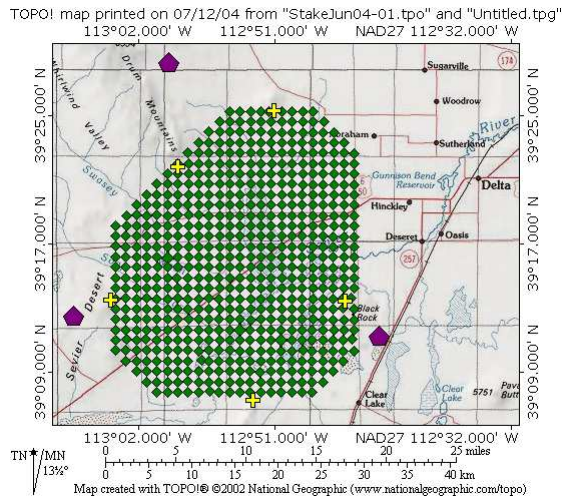


Figure 1. Detector arrangement of the TA SDs (*diamond*) and the FD stations (*pentagon*).

## 2. Surface Detector

The surface detectors are distributed on a 1.2 km square grid and the effective detection area of the whole SD array will be 762 km<sup>2</sup>. Each SD (Figure 2) has an assembled weight of 250 kg and consists of a power supply, two layers of scintillation detector and electronics. Power is generated by a 120 W solar panel and stored in a sealed lead-acid battery. The system has the capacity for one week’s operation in complete darkness.

Each scintillation detector layer is made of extruded plastic scintillator 1.2 cm thick and with an area of 3 m<sup>2</sup>. The photo multiplier tube (PMT, Electrontube 91245A with 9/8 inch diameter) is connected to the scintillator via 96 wave length shifting fibers (WLSFs, 2mm diameter). The fibers rest in grooves in the scintillator

\*Corresponding Author: S. Ogio, sogio@sci.osaka-cu.ac.jp



Figure 2. A surface detector deployed in the field.

aligned parallel to the long side of the scintillator panels and have 2 cm separation. The averaged number of photo electrons induced by a penetrating Minimum Ionizing Particle (MIP) is 24. The PMT is set to a gain of about  $4 \times 10^6$ .

The analog part of the SD electronics[7] has an low-pass filter with cut-off frequency of 9.7 MHz for each PMT, and the output is readout by a 50 MHz 12 bit FADC. The ADC delivers its data to a buffer which has sufficient capacity to store data for 16,000 events at  $5.12 \mu\text{s}/\text{event}$ .

The event trigger for the SD array is implemented in a Field Programable Gate Array (FPGA). At present, we intend to use the three fold coincidence of nearby detectors with more than three particle hits. In this case, the trigger recognition time is less than 10 ms. Using the above triggering conditions, we calculated the triggering efficiencies for UHECRs which have incident zenith angles less than  $45^\circ$ . The efficiency for primary protons is 35% at an energy of  $10^{18}$  eV and 100% at  $10^{19}$  eV. The estimated energy resolutions from analyzing simulated events is about 27% at  $10^{19}$  eV and 19% at  $10^{20}$  eV, which comparable in accuracy to AGASA.

### 3. FD Station, Telescope and Camera

The Telescope Array consists of three Fluorescence Detector (FD) stations. The stations are

located on a triangle with about 35 km separation and consists of 12-14 telescopes. Each station is centered on the central laser facility in the middle of the array and views  $3^\circ$ - $33^\circ$  in elevation and  $\sim 108^\circ$  in azimuth, and thus each one views nearly the entire array at high energies.

We have completed installation of telescopes at the first FD station in the south-east corner of the array, and we are currently installing the telescopes at the second station in the south-west corner. The third station near the north-west corner is currently under construction. The site will be complete by the end of 2006 and we plan to move some of the HiRes-I telescopes to this station.

The telescopes (Figure 3) at the first two sites have a combined spherical mirror with a diameter of 3.3 m, a focal length of 3.0 m and a spot size of 30 mm on the focal plane. The pointing accuracy of the telescopes is  $0.07^\circ$ .

Each telescope has a fluorescence light camera which consists of 256 PMTs (HAMAMATSU R9508). The sensitive area of the camera is  $1 \text{ m} \times 1 \text{ m}$ , which corresponds to the field of view of  $15^\circ$  in elevation times  $18^\circ$  in azimuth. Thus the pixel size of the camera is nearly equal to  $1^\circ$ .

The high voltage to the PMT is negative and is applied to the PMTs individually with a computer controlled power supply system. This allows us to match the gains of all the PMTs and to compensate for aging effects of the PMTs. Moreover, the PMTs are DC-coupled so that the direct measurement of the DC-anode current of night sky background at the front-end electronics is possible.

In each camera three PMTs among the 256 are absolutely calibrated with a standard light source called ‘‘CRAYS’’ [8], which exposes PMTs to Rayleigh-scattered photons out of a calibrated  $\text{N}_2$  laser (337.1 nm,  $300 \mu\text{J}$ ) in a  $\text{N}_2$ -filled chamber. Moreover, the gain of each calibrated PMT is monitored through the constant measurements using a YAP light pulsar attached on the photo cathode. The YAP pulsar[9] consists of  $^{241}\text{Am}$  and a  $\text{YAIO}_3:\text{Ce}$  scintillator, and its dimension are 4 mm in diameter and 2 mm in thickness. The gains of other PMTs are calibrated relative to the absolutely calibrated PMTs by comparing

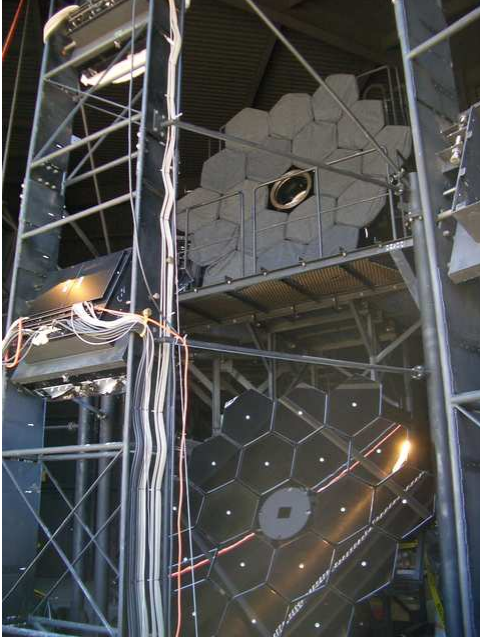


Figure 3. Telescopes and cameras in the first TA FD station. Every segment mirror of the upper mirror has a cover to avoid dust.

output signals of PMTs when they are exposed to a Xe flasher installed at the center of a mirror. The accuracy of absolute and relative gain determinations is 7% and 2.5%, respectively. Finally, the PMT-gain is set at  $8 \times 10^4$  and the gain of the pre-amplifiers at the PMTs is 50.

#### 4. FD Electronics

The schematic of the electronics and the data acquisition (DAQ) system of a FD station is shown in Figure 4. The FD electronics[10] consists of the following three main components: the Signal Digitizer/Finder (SDF), the Track Finder (TF), and the Central Trigger Distributer (CTD). Each component fits on a single width VME-9U module.

Each SDF board processes the signals of one camera column, *i.e.*, there are 16 channels per board. Each channel has a FADC to readout

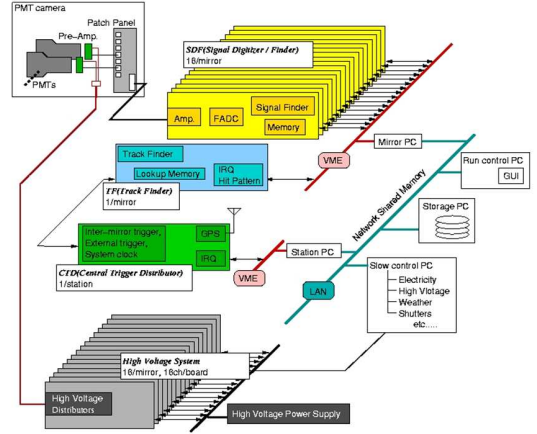


Figure 4. A block diagram of the electronic and the DAQ system in a FD station.

the pre-amplifier, a buffer memory, and a signal finder logic. The analog input is split into a low gain (1/16) sum per 16 channels. The sum channel also has a FADC and a buffer memory. With the sum channels, the effective dynamic range and the sampling frequency of SDF is equivalent to 16 bits at 10MHz. The signal finder logic measures the significance of the excess photons above night sky background in every  $12.8 \mu\text{s}$  window, which we call “frames”. In a frame, the sum of ADC values of the first  $N$  samples are compared with the fluctuation of DC current which is calculated from the last 125 frames. This is processed for four different sum window size  $N = 16, 32, 64$  and 128, and the recognitions are repeated with shifting the sum window by 1 sampling time until the window reaches the end of the frame. In these processes, when the net count which is the averaged DC current from the sum exceeds a threshold, this channel is recognized as a “hit” channel in the frame. The threshold of the significance level is programmable. The time for the signal finding in a frame is  $1.8 \mu\text{s}$ .

Each TF processes the hit patterns of one camera in every frame. The TF recognizes 5-fold hit pixel patterns as a track and 4-fold hit on the edge of the camera as a partial track, and sends

the track recognition result to the CTD. The processing time for single track finding routine is  $5.4 \mu\text{s}$ .

One CTD processes the track recognition results of whole the camera in a FD station. When one or more TFs find tracks, CTD distributes trigger signals to start data recording procedures for all the SDFs and the TFs. Moreover, when each of two neighboring TFs finds a partial track, the CTD also triggers the DAQ system. The total triggering time including SDF and TF processing is  $9.8 \mu\text{s}$ . In addition, the CTD takes care of other important functions – such as tracking the GPS clock, external trigger input, synchronization of the system clock for all the electronics of the DAQ system in a station.

The triggering efficiencies of the FD stations for stereo coincidence are shown in Figure 5. In the energy range of  $10^{19}$  eV and above the detection area of stereo FD almost completely covers the SD array.

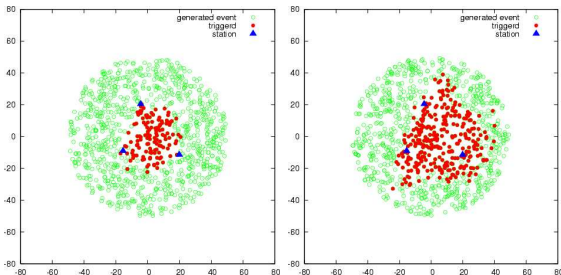


Figure 5. The core locations of the incident cosmic rays (*green open circle*) and the stereo-triggered showers (*red filled circle*) for primary protons of an incident zenith angle of  $30^\circ$ . The primary energies are  $10^{19}$  eV (*left*) and  $10^{20}$  eV (*right*). Each of the blue filled triangles indicates a location of a FD station.

The DAQ computers are twelve Mirror PCs, a Station PC for CTD, a Slow Control PC, a Data Storage PC, an Analysis PC and a GUI PC. We use the Linux operating system for every

PC and use a Network Shared Memory (NSM) library which was developed for the DAQ system of the Belle experiment at KEK. This library provides PC to PC communication services similar to “signal” and “shared-memory” on UNIX. The data size per event is 250 kB per camera. Consequently, the amount of data per night is 10 GB per station, when the triggering rate is 1.2 Hz per station. We will expect to regulate the SDF threshold level to keep the trigger rate at about 1 Hz per station, because the expected air shower event rate is 0.005 Hz. However, the DAQ system has the potential to work with a maximum rate of 20 Hz.

## 5. Atmospheric Monitoring and Calibrations

In order to monitor the condition of the atmosphere, we use two monitoring systems. The first is a steerable laser (used in bi-static LIDAR mode) which is located at the Central Laser Facility (CLF). This provides a “test beam” to investigate properties of the atmosphere and the FDs. The CLF is located at the center of the array and is equidistant from each FD station (20.85 km). The CLF laser is an energy tripled Nd:YAG laser ( $\lambda = 355$  nm) with an output of 5 mJ. Thus, at a full energy, the number of photons out of a beam is  $3.8 \times 10^{11}$  photons/m which is approximately equivalent to fluorescence photons emitted by showers with energy of  $10^{20}$  eV, *i.e.*, about  $4 \times 10^{11}$  photons/m.

The second atmospheric monitoring system is a standard LIDAR system[11]. It consists of a laser and light detectors to measure the intensity and the time profiles of back scattered photons. One such station will be installed at each of the FD stations. The LIDAR at the first FD station has a Nd:YAG laser (355 nm) with an output of 5 mJ and a photon detector which consists of a f/10 Cassegrain-telescope with a diameter of 30.5 cm and a PMT with a diameter of 19 mm.

For an end-to-end calibration of FDs, we have a plan to use a linear electron accelerator (40 MeV/electron) in a trailer. We will shoot the accelerator vertically in the FD’s field of view at a distance of 100 meters. The current from the

accelerator is  $10^9$  electrons per shot and the repetition frequency is 1 Hz. The amount of energy in one shot of the LINAC is  $4 \times 10^{16}$  eV, which is equivalent to  $10^{20}$  eV at a distance of 10 km. If we can use this “test beam” calibration, we will reduce the energy determination uncertainty of 20% to 14% including the uncertainty due to atmospheric monitoring.

## 6. Conclusion

The Telescope Array Project is under construction in central Utah, USA. The Surface Detectors are being deployed and the array should be complete by the end of February, 2007. The first of three Fluorescence Detector stations is nearly complete. The building for the second is complete and the site should be operational in 3/2007. The Third site is under construction and should be operational in 5/2007. We will soon be collecting hybrid data at the Telescope Array.

## 7. Acknowledgments

The Telescope Array collaboration wishes to acknowledge the support of the the Japanese government through a Grant-in-Aid for Scientific Research (Kakenhi) on the Priority Area “The Origin of the Highest Energy Cosmic Rays” as well as the U.S. National Science Foundation (NSF) through awards PHY-0307098 and PHY-0601915 (University of Utah) and PHY-0305516 (Rutgers University). The Dr. Ezekiel R. and Edna Wattis Dumke Foundation, The Willard L. Eccles Foundation and The George S. and Dolores Dore Eccles Foundation all helped with generous donations. The State of Utah supported the project through its Economic Development Board, and the University of Utah supported us through the Office of the Vice President for Research. We gratefully acknowledge the contributions from the technical staffs of our home institutions and the Utah Center for High Performance Computing. The TA could not be built without strong support from the agencies that administer the lands and airspace above our project area. We thank the State of Utah School and Institutional Trust Lands Administration, the federal Bureau

of Land Management, and the United States Air Force. We also wish to thank the people and officials of Millard County, Utah, for their steadfast support of our experiment.

## REFERENCES

1. <http://www.telescopearray.org>
2. M.Takeda et al., Phys. Rev. Lett. 81 (1998) 1163
3. M.Takeda et al., Ap. J. 522 (1999) 255
4. R.U. Abbasi et al., Astroparticle Phys. 23 (2005) 157
5. H. Kawai et al., Proc. of 29th ICRC 8 (2005) 181
6. H.J. Drescher, A. Dumitru and M. Strikman, Phys. Rev. Lett. 94 (2005) 231801; H.J. Drescher, Proc. of 29th ICRC 7 (2005) 95
7. Y. Hayashi et al., Proc. of 29th ICRC 8 (2005) 161; S. Ozawa et al., Proc. of 29th ICRC 8 (2005) 177
8. H. Tokuno et al., Proc. of 29th ICRC 8 (2005) 221
9. M. Kobayashi et al., Nucl. Inst. and Meth. A337 (1994) 355
10. A. Taketa et al., Proc. of 29th ICRC 8 (2005) 209; Y. Tameda et al., Proc. of 29th ICRC 8 (2005) 225
11. M. Chikawa et al., Proc. of 29th ICRC 8 (2005) 137